The Zinc-Finger Protein Slug Causes Desmosome Dissociation, an Initial and Necessary Step for Growth Factor–induced Epithelial–Mesenchymal Transition

Pierre Savagner,*‡ Kenneth M. Yamada,‡ and Jean Paul Thiery*

*Centre National de la Recherche Scientifique–Institut Curie, 75231 Paris Cedex 05, France; and ‡Craniofacial Developmental Biology and Regeneration Branch, National Institute of Dental Research, National Institutes of Health, Bethesda, Maryland 20892-4370

Abstract. Epithelial–mesenchymal transition (EMT) is an essential morphogenetic process during embryonic development. It can be induced in vitro by hepatocyte growth factor/scatter factor (HGF/SF), or by FGF-1 in our NBT-II cell model for EMT. We tested for a central role in EMT of a zinc-finger protein called Slug. Slug mRNA and protein levels were increased transiently in FGF-1–treated NBT-II cells. Transient or stable transfection of Slug cDNA in NBT-II cells resulted in a striking disappearance of the desmosomal markers desmoplakin and desmoglein from cell–cell contact areas, mimicking the initial steps of FGF-1 or HGF/SF-induced EMT. Stable transfectant cells expressed Slug protein and were less epithelial, with increased cell spreading and cell–cell separation in subconfluent cultures. Interestingly, NBT-II cells transfected with antisense Slug cDNA were able to resist EMT induction by FGF-1 or even HGF/SF. This antisense effect was suppressed by retransfection with Slug sense cDNA. Our results indicate that Slug induces the first phase of growth factor–induced EMT, including desmosome dissociation, cell spreading, and initiation of cell separation. Moreover, the antisense inhibition experiments suggest that Slug is also necessary for EMT.

EPITHELIAL cells adhere to each other through specialized structures essential for the maintenance of epithelial organization and differentiation. Among these, structures linked to the cytokeratin intermediate filament network appear to provide the strongest and most resilient adhesion (12, 15). The core unit of such structures is the desmosome, which appears early during epithelial differentiation (13, 24, 30, 37). Desmoglein and desmocollins are desmosome-specific cadherins that mediate cell–cell binding (15, 34). They are part of a molecular complex involving γ-catenin/plakoglobin, Band 6/plakophilin, and desmoplakin, among other components (26, 29, 40, 56, 57, 62–64). Desmoplakin can bind directly to cytokeratin filaments in vitro and appears to enhance desmosome stability (35, 56, 57). Studies with dominant-negative variants indicate that desmoplakin is required in vivo for attaching intermediate filaments to the desmosome (4). Little is known, however, about how desmosomal assembly is regulated.

Individualization of cells emerging and dissociating from an epithelial sheet is one of the basic mechanisms involved in embryonic development. In early postimplantation mouse embryos, it appears that all cells that contribute to embryonic tissues are epithelial cells expressing desmosomes (30). Therefore, cellular dissociation involves the disintegration of these desmosomes and other cell–cell adhesion systems. Depending on the species, this necessary process of epithelial–mesenchymal transition (EMT)[1] occurs at several critical stages during development, such as gastrulation, neural crest cell emigration, and organogenesis (for reviews see references 19, 27, 28, 38, 52).

Several inducers, including extracellular molecules (5, 32, 33, 50, 54, 67, 68) and growth-factors from the transforming growth factor (TGF)β and FGF families (10, 47), have been suggested to play a role during these embryonic phenotype modulations. Transcription factors are likely to be involved at some point during the process. For example, the zinc-finger protein Slug was found to be expressed in chicken neural crest cells just before they emerge from the neural tube and later during their migration phase (46). Interestingly, the same report described Slug expression by epiblast cells lining the primitive streak during gastrulation, just before the emergence of mesenchymal cells. Treatment of developing embryos with antisense oligonu-

Address all correspondence to Pierre Savagner, Craniofacial Developmental Biology and Regeneration Branch, NIDR, Bldg. 30, Rm. 424, 30 Convent Drive MSC 4370, National Institutes of Health, Bethesda, MD 20892-4370. Tel: (301) 496-6040; Fax: (301) 402-0897.

1. *Abbreviations used in this paper*: EMT, epithelial-mesenchymal transition; HGF/SF, hepatocyte growth factor/scatter factor; IL-2R, interleukin-2 receptor; MDCK, Madin-Darby canine kidney.

cleotides from *slug* was found to interfere with these two processes, suggesting a potential causal role for Slug in the EMT process in vivo. Slug and closely related members of the Snail family were also found to express similar patterns of localization in *Xenopus* and zebrafish embryos, providing an early marker for neural crest cells.

Epithelial cells can be induced to dissociate by treatment with hepatocyte growth factor/scatter factor (HGF/SF), and in some cases by other growth factor members of the FGF (65), EGF, and TGF families (3, 16, 43). The EMT process is initiated by cell–cell dissociation, which is preceded by the internalization of desmosomal components and progressive disappearance from cell–cell contact areas (7). As studied in Madin-Darby canine kidney (MDCK) cells, these scatter factors can also act as growth factors and morphogenetic factors, using specific transduction pathways in each case (1, 17, 25, 51, 58).

We have previously characterized a rat bladder carcinoma cell line, NBT-II, that is induced by FGF-1 to undergo an EMT characterized by a switch to a fibroblastoid phenotype and by cell migration (7, 65). Desmosomal components, including desmoplakin and desmoglein, were found to be internalized and disappear from the surface starting 4 h after initiation of FGF-1 treatment. By 6 h, >50% of the cells no longer express desmosomes. By 12 h, cells undergo active migration on the substrate (7). In contrast, adherens junction components such as E-cadherin and catenins were not altered quantitatively during this epithelial–mesenchymal transition (8). However, E-cadherin was redistributed from cell–cell contact areas to a diffuse distribution on the cell surface. FGF-1 activation was mediated through the receptor FGFR2c/KGFR, which underwent alternative splicing during the EMT process (53). The FGFR2c/KGFR tyrosine kinase domain was found to be involved in transducing the EMT process through phosphorylation (6). In addition, an EMT-specific activation of $pp60^{c\text{-}src}$ was demonstrated (49), and overexpression of normal c-src in NBT-II cells was found to oversensitize them to EMT induced by FGF-1. Transcriptional and translational events were also found to be required for EMT since actinomycin D inhibited EMT (Savagner, P., unpublished observation), as did cycloheximide (8).

Prompted by the developmental studies cited above, we investigated the role and cell biological effects of the zinc-finger protein Slug in FGF-1–induced EMT in NBT-II cells, extended our studies to HGF/SF, and tested for a potential direct role for Slug in inducing EMT.

Materials and Methods

Reagents

Human recombinant FGF-1 was kindly provided by Dr. M. Jaye (Rhône Poulenc Rorer Central Research Inc., King of Prussia, PA). HGF/SF was purchased from PeproTech (Rocky Hill, NJ). Mouse monoclonal antibodies against bovine desmoplakins 1 and 2 (clone DP 2.15, 2.17, and 2.20) and bovine desmoglein ("band 3": Clone DG 3.10) were purchased from American Research Products (Solon, OH). Monoclonal antibodies against E-cadherin (Clone 34) were purchased from Transduction Laboratories (Lexington, KY). Monoclonal antibodies against human vimentin (clone V 9) and bovine cytokeratins (pan-cytokeratin) were purchased from Zymed Labs (S. San Francisco, CA). Mouse antibodies against chicken Slug (39) were a gift from Dr. T. Jessell (Columbia University, New York).

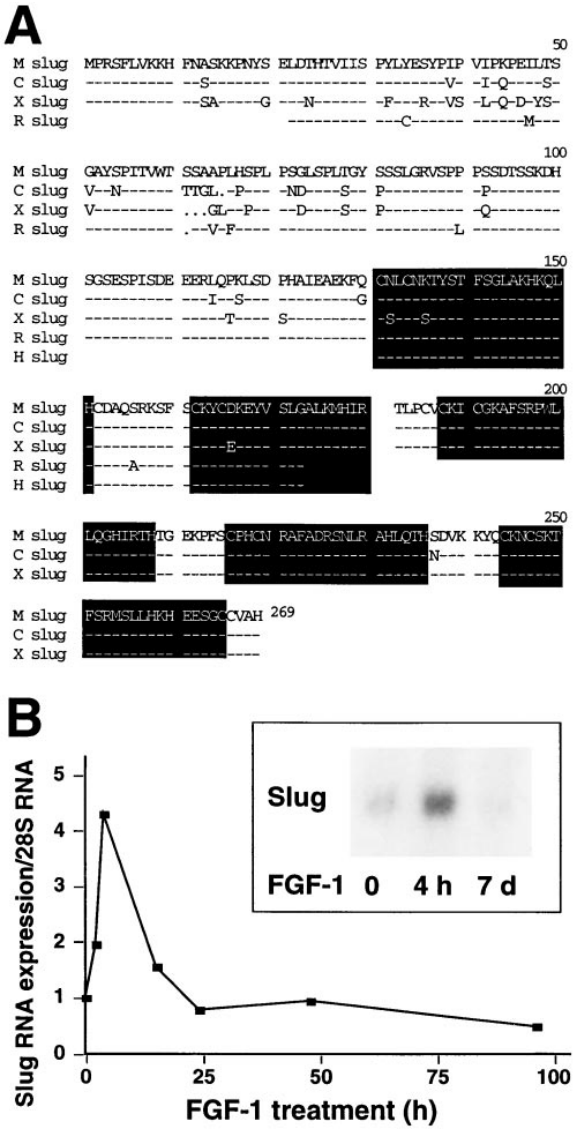

Figure 1. (*A*) Comparison of mouse, rat, and human sequences of Slug cDNA. The mouse Slug (*M slug*) cDNA was isolated from a mouse cDNA library. Rat (*R slug*) and human (*H slug*) PCR P64-P41 and P57-P41 fragments were amplified by PCR using primers P57, P64, and P41. Sequences were aligned with chick (*C slug*) and *Xenopus* (*X slug*) Slug sequences, highlighting the five zinc-finger domains. These sequence data are available from GenBank/EMBL/DDBJ under accession numbers U97059, U97060, and U97061. (*B*) Northern analysis of Slug expression in NBT-II cells. NBT-II cells were treated with FGF-1 (20 ng/ml) for the time periods indicated. RNA was separated on a formaldehyde-agarose gel, subsequently transferred to a Nylon membrane and hybridized with the *slug* fragment P64-P41 probe, and then, after washing, was reprobed with a ribosomal 28S probe. Slug relative expression was normalized in both cases to the basal level of Slug expression ($t = 0$) and the corresponding level of 28S RNA to define the time course shown on the graph. Insert displays a different Northern analysis experiment showing a similar transient expression pattern. Northern analysis was repeated in five independent experiments and gave similar results.

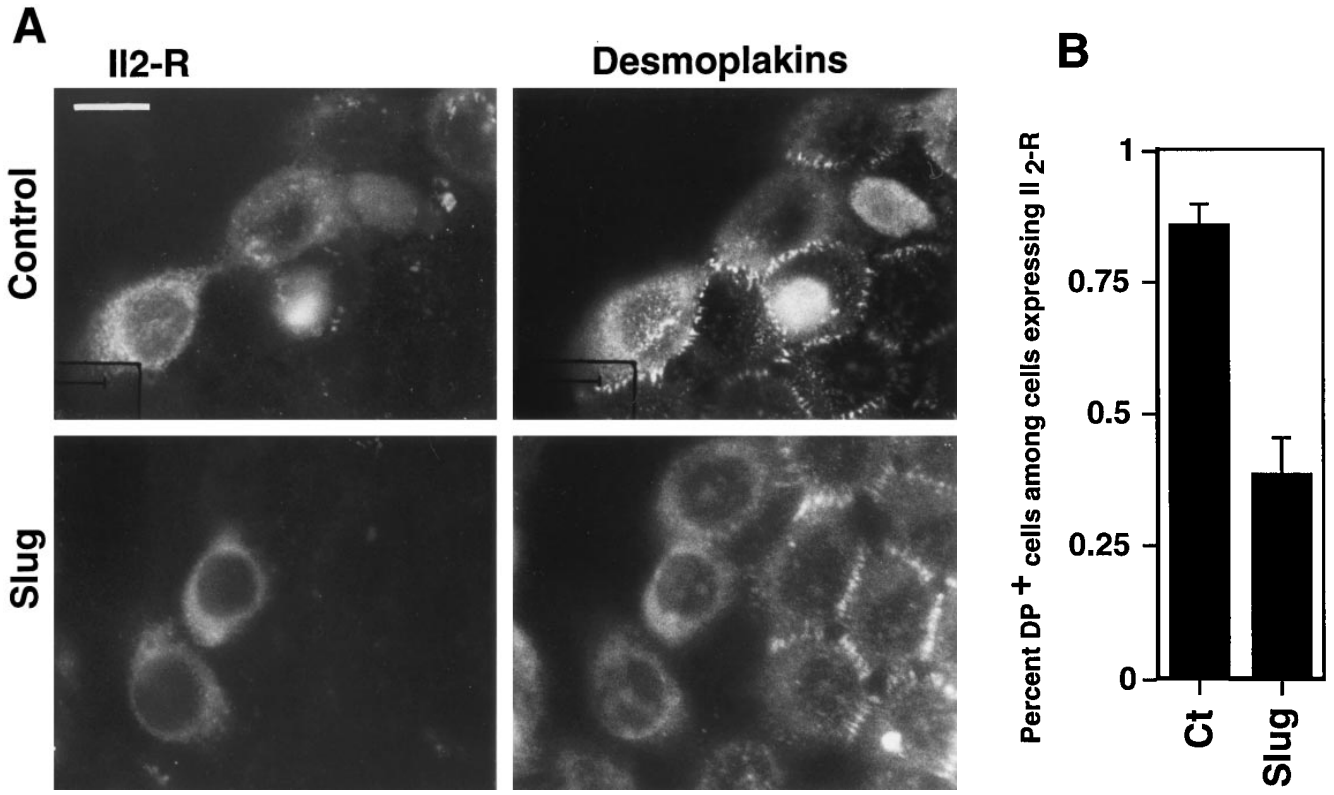

Figure 2. Slug transient transfections. NBT-II cells were cotransfected with vectors containing mouse full-length cDNA for Slug and a truncated (IL-2R) cDNA used as a transfection marker. Alternatively, a control vector pCR 3 (*Control*) was cotransfected with IL-2R cDNA. After 48 h, cells were fixed and processed for double immunofluorescence using antibodies against IL-2R and antidesmoplakin (*A*); note that cells expressing the IL-2R transfection marker are positive for desmoplakin in control transfectants and negative in *slug*-transfected cells. Cells expressing desmoplakin at cell–cell boundaries were counted as desmosome-positive (DP^+), i.e., fully epithelial. More than 100 cells expressing IL-2R were analyzed at the same time point for desmosome expression. The number of desmosome-positive cells displaying IL-2R labeling was normalized to the total number of cells expressing IL-2R (*B*). Bar, 9 μm.

Cell Culture

The rat bladder carcinoma NBT-II cell line was initially obtained from Prof. Marc Mareel (University Hospital, Ghent, Belgium). Cells were cultured in DME supplemented with glutamine, antibiotics, and 10% heat-inactivated FCS as previously described (7). Human keratinocyte primary culture YF29 (newborn foreskin, fourth passage) was grown by A. Rochat and Y. Barrandon (Ecole Normale Supérieure, Paris, France) in DME supplemented with glutamine, antibiotics, and 10% heat-inactivated FCS.

RNA Preparation and PCR

Total RNA was extracted from human keratinocytes and NBT-II cells that were growth-arrested by serum deprivation and incubated in serum-containing medium for 6 h by the acid guanidinium thiocyanate-phenol method (11). Synthesis of cDNA was performed using AMV reverse transcriptase as specified by the supplier (Stratagene, La Jolla, CA). The total volume for each reaction was 100 μl for 4 μg of RNA. PCR reactions included 5 μl of cDNA as template, 0.4 μg of each specific primer, 0.2 mM dNTPs, and 2 U of Taq polymerase in a buffer supplied with the enzyme (Perkin-Elmer Corp., Norwalk, CT). Annealing temperature was 46°C.

Primers

Specific primers were designed based on a published chicken Slug sequence (46) and mouse Snail sequence (45, 55). The primer sequences were P41: CTTCGGATGTGCATCTTCAGAC (Mouse Snail bp 744–764), P57: AT(ACT)GA(AG)GC(ACGT)GA(AG)AA(AG)TT(TC)CA(GA)TG (chicken Slug, amino acids 125–131), P64: AAGCCCAACTATAGCGAGCTG (mouse Snail bp 46–66), P85: CTTGTAGTCGGATCCGTGTGCCACACAGCAGCCAGA (Mouse Slug 3′ end), and P86: TCGAATTCGCGGTCGCTGTC.

Cloning and Sequencing

The PCR fragments P57-P41 and P64-P41 obtained from human keratinocyte cDNA, NBT-II cell cDNA, and a mouse cDNA library derived from the putative neural crest cell line NC15 (a gift from Dr. Karen Brown, National Institute of Dental Research) were cloned in PCR II (Invitrogen, San Diego, CA) and sequenced using an automated DNA sequencer. The PCR fragment S64-41, obtained from a mouse cDNA library, was cloned in the PCR II vector and used as a probe for screening a mouse cDNA library (kindly provided by Dr. Karen Brown) that was based on λZAP II (Stratagene). A clone was excised in pBluescript and sequenced in both directions using an automated DNA sequencer and various primers derived from successive sequencing. Slug expression vectors were prepared by cloning the mouse PCR product P86-P85 containing the full-length mouse *slug* sequence in a PCR 3 vector (Invitrogen). The interleukin-2 receptor (IL-2R) expression vector was described previously (36). Sequences were analyzed using the Wisconsin package (Genetics Computer Group, Madison, WI) and Mac Vector (Oxford Molecular Group, Campbell, CA) software.

Transfection and Cell Selection

Expression vectors containing full-length mouse *slug* sequence were transfected into NBT-II cells plated in 16-well slide chambers (Nunc) with 0.25 μl lipofectamine (Life Technologies, Grand Island, NY). For transient transfections in NBT-II cells, 0.1 μg of IL-2R construct was added during the transfection to serve as a marker for transfection (20). Wells were washed several times after 6 h of incubation. NBT-II cells were cultured for an-

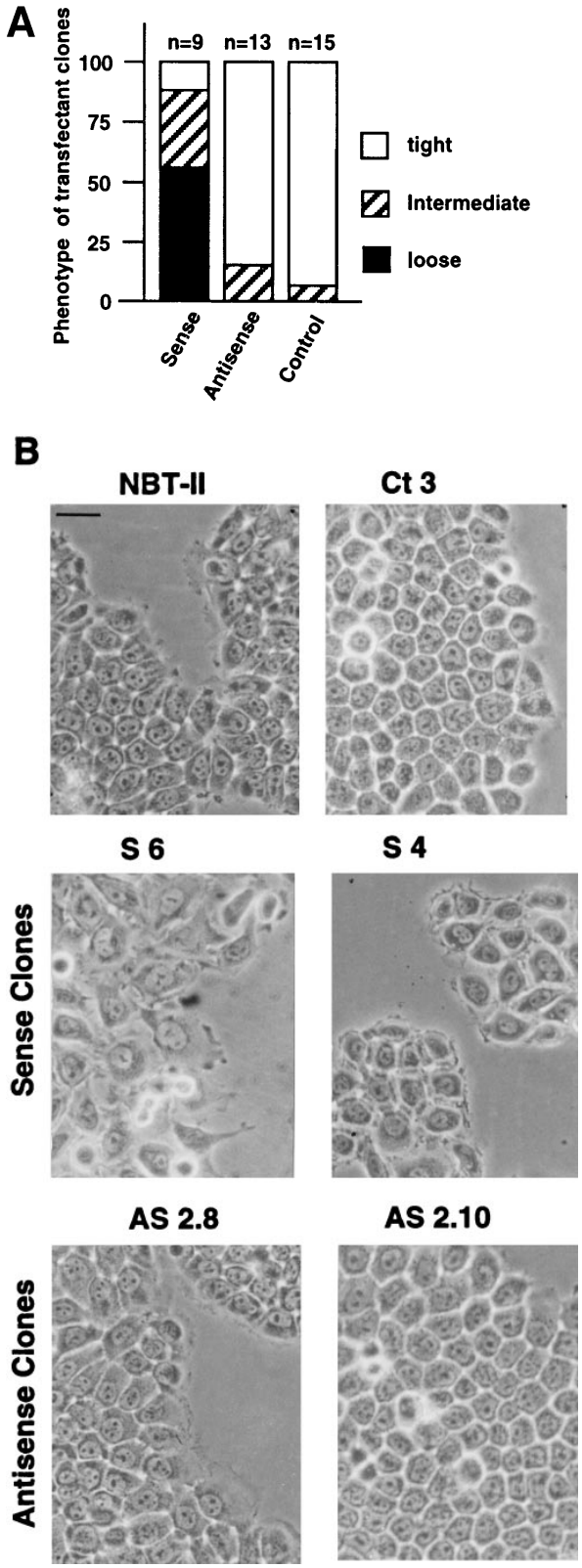

Figure 3. *slug*-transfected cells display a modified morphological phenotype. After selection and cloning, stable transfectant clones were cultured under standard conditions. (*A*) Phenotype expression of stable *slug* transfectants, comparing sense, antisense, and control clones. 37 clones were analyzed by phase-contrast microscopy for their phenotype and classified according to the appearance of cell–cell junctions as tight, intermediate, and loose. (*B*) Phase-contrast micrographs of sense (S6 and S4) and antisense (AS2.8 and AS2.10) *slug* transfectants were taken after 48–72 h of cell culture. The morphology of the cell junctions in S4 and S6 were classified as loose, whereas the other four were classified as tight for quantification for *A*. Bar, 10 μm.

other 48 h before fixation. For stable transfections, NBT-II cells were incubated with DNA/lipofectamine for 15 h, washed repeatedly, and then treated with 400 μg/ml active G418 (Life Technologies) for 7 d. Surviving cells were cloned individually by limiting dilution.

Immunofluorescence Microscopy

Cells cultured on 16-well multiwell glass slides (Nunc) were treated with FGF-1 for 2 d after cell plating. Heparin (Choay Laboratories, Paris, France) at 10 μg/ml was added to the culture medium to stabilize the biological activity of FGF-1 (22). Growth factors were renewed every other day for long term activation. NBT-II cells were processed for immunocytochemistry as described previously (8).

Electron Microscopy

Cells were cultured for 72 h before fixation in 2% glutaraldehyde, 2% paraformaldehyde in cacodylate buffer. After postfixation in 1% osmium tetroxyde, they were progressively dehydrated in ethanol and then lifted from the culture dishes before embedding in Epon resin. Ultrathin sections were stained with 2% uranyl acetate and 1% lead citrate before visualization with a transmission electron microscope (JEOL; Tokyo, Japan).

Nucleus-to-Nucleus Distance

High-magnification photographs were measured with a ruler to find the distance from the geometrical center of nuclei from adjacent cells. More than 50 measurements were done in each case. Adjacent cells were chosen randomly, and cells located at the edges of aggregates were excluded.

Motility Assays

Motility assays were performed using cells seeded on plastic tissue culture dishes and cultured for 2 d in standard medium. Dishes were covered with a glass slide, and time-lapse video cinematography was performed over 15 h after addition of growth factor. The average speed of locomotion was calculated from more than 30 distinct cell tracks chosen randomly. For each cell, total cell migration distance during the time of migration (5–6 h) was determined.

Northern Analysis

After separation on a 1.2% formaldehyde–containing agarose gel, RNAs were transferred overnight to a Nylon membrane (Nytran; Schleicher and Schuell, Keene, NH). The P64-P41 *slug* probe was excised from PCR II constructs and a ribosomal human 28S probe was excised from HHCD07 (American Type Culture Collection, Rockville, MD). Both probes were [^{32}P]dCTP-labeled using a Primer II kit (Stratagene) and then incubated overnight at 42°C with filters in hybridization solution (5× SSC, 5× Denhardt's, 50% formamide, 10% dextran sulfate, 50 μg/ml salmon sperm DNA, and 0.4% SDS). After washing twice for 10 min at 42°C in 0.25× SSC and 0.1% SDS, filters were dried and exposed to Hyperfilm-MP (Amersham Corp., Arlington Heights, IL) for 2 d. Quantitation was performed using a PhosphorImager (Molecular Dynamics, Sunnyvale, CA).

Results

Cloning and Sequence Analysis of Mammalian Slug cDNA

We cloned by PCR several Slug cDNA fragments using primers derived from the chick sequence. We used the fragment P64-P41, amplified with primer set 64/41 to screen

a mouse cDNA library. We obtained a full-length mouse Slug cDNA clone; its deduced amino acid sequence is shown in Fig. 1. This clone has 92% amino-acid identity with the chicken Slug sequence. It includes the "trademark" MPRSFLV K/R K amino-terminal sequence characteristic of the Snail family (42, 46, 61). As in chicken Slug, it contains four classic CXXC (12 X) HXXXH zinc-fingers and a fifth one representing a structural variant apparently specific for the Snail family: CXXXC (12 X) HXXXXC (61). As noted for *Xenopus*, mouse Slug is very similar (90% identity) to the mouse Snail protein in the carboxy-terminal half of the molecule after amino acid 160. This region includes the four zinc-finger domains expressed by the mouse Snail gene.

Amplification products derived from the 57/41 or 64/41 primer sets were also cloned and sequenced from human keratinocytes and rat bladder carcinoma cells (NBT-II). Interestingly, the mouse amino acid sequence in this region, covering the first two zinc-finger domains, was 100% identical to the sequence of the human Slug clone and 98% identical to the sequence of the rat clone (Fig. 1).

Slug mRNA Expression Rises Early after FGF-1 Treatment

RNA was extracted from NBT-II cells at various times after EMT-triggered FGF-1 treatment. The *slug* fragment S64-41 was labeled with ^{32}P and used for Northern blot analysis. As shown in Fig. 1, Slug RNA was induced as early as 3 h after FGF-1 treatment. Expression reached a peak at 6 h and then decreased after 15 h. Under these conditions, NBT-II cells cultured with FGF-1 for more than 6 d no longer expressed Slug mRNA.

Slug-transfected Cells Display a Modified Phenotype

The full-length cDNA encoding mouse *slug* was inserted in both orientations in the expression vector PCR 3 under the control of a cytomegalovirus promoter. Constructs were cotransfected transiently into NBT-II cells using lipofectamine together with an expression vector encoding a truncated IL-2R described as a marker for DNA uptake and expression (20, 36). Desmoplakin immunolabeling was used to localize desmosomes. As described previously (65), untreated parental NBT-II cells have a localization of desmoplakin at punctate sites corresponding to desmosomes, which is restricted to cell–cell contact areas. However, this pattern disappears when cells are induced to undergo EMT with FGF-1, and cells treated for >12 h with FGF-1 are devoid of desmosomes. To examine for similar modulation in the transiently transfected cells, we counted 100–200 cells displaying IL-2R labeling for each condition. We then calculated the proportion of desmoplakin-positive cells among the cells expressing the IL-2R. Cells cotransfected with Slug cDNA were compared to cells cotransfected with the control vector PCR 3 (Fig. 2). The proportion of cells displaying desmosomes after *slug* transfection was less than half that of control-transfected cells, and this difference was highly significant ($P < 0.004$).

Since transient transfections indicated a Slug-mediated modulation of cell phenotype, we established clones of stable transfectants with Slug cDNA in either orientation together with a Neomycin resistance gene to produce sense and antisense transfectants, as well as transfecting with expression vector alone. Cells were selected in the presence of Geneticin (G 418) and cloned individually by limiting dilution. A total of 37 independent transfectant clones including 9 controls, 13 antisense clones, and 15 sense clones were established and analyzed. *slug* (sense and antisense)–transfected cells, as well as control-transfected cells, displayed cell–cell associations classified as tight, intermediate, or loose according to their morphology (Fig. 3 *A*). "Tight" cell contacts were defined in this system as sites visualized by phase-contrast microscopy as simple phase refractile (bright) lines, outlining flat apical areas of epithelioid cells. "Loose" cell contacts showed a much more complex pattern at cell–cell contact areas, with irregular cell–cell boundaries that often showed phase-refractile zones at flattening surfaces of cells that were internal to phase-dark zones at flat sites of variable cell–cell contact. When the cell population phenotype was heterogeneous, cells were considered to display an intermediate morphology. In subconfluent cultures, the normal pattern of NBT-II cell distribution, in which clusters of cells organize themselves into closely packed epithelial islands surrounded by empty spaces, was replaced by a modified phenotype in *slug*-transfected cells, in which cell–cell associations appeared much looser. Two sense clones, S4 and S6, are shown in Fig. 3 *B*. They show a modification of cell–cell contact areas that is particularly apparent at higher magnification (Fig. 4 *A*), with a wider cell–cell junction area or separations at cell junctions that disrupted the more cuboidal epithelial pattern of parental NBT-II cells. The proportion of the cell periphery involved in contact with another cell was substantially decreased. Cells located within the interior of groups of cells had >90% of their peripheral membrane in contact with an adjacent cell, whereas cells transfected with the sense *slug* construct had only 46% of their membrane in contact, as estimated from photographs. As a consequence, there were spaces of varying size in the monolayer even when adjacent cells were in contact (Fig. 4 *A*).

To study in detail the nature of the cell–cell contact areas, S6 and untransfected NBT-II cells were examined in electron microscopy. NBT-II cells were found to exhibit characteristic morphological features of epithelial cells such as desmosomes (Fig. 4 *B*) and putative adherens junctions (data not shown). They displayed numerous interdigitating processes, similar to those reported in bladder epithelial cells in vivo (9). In contrast, the Slug sense clone cDNA S6 showed flattened and spread cells devoid of desmosomes, still in contact with each other through much more limited lateral contact areas (Fig. 4 *B*). Interdigitating processes similar to those in untransfected cells were found, as well as putative cell adherens junctions (data not shown).

Phenotype modulation was also characterized by an increased spreading apart of the transfected cells on the substrate. To quantify this alteration, we calculated the average nucleus-to-nucleus distance in the stable transfectants. We found that sense clone S6 displayed twice the nucleus-to-nucleus distance as compared to the parental NBT-II cells or to the antisense-transfected cells (Fig. 4 *C*). On the other hand, antisense-transfected clones such as AS2.8

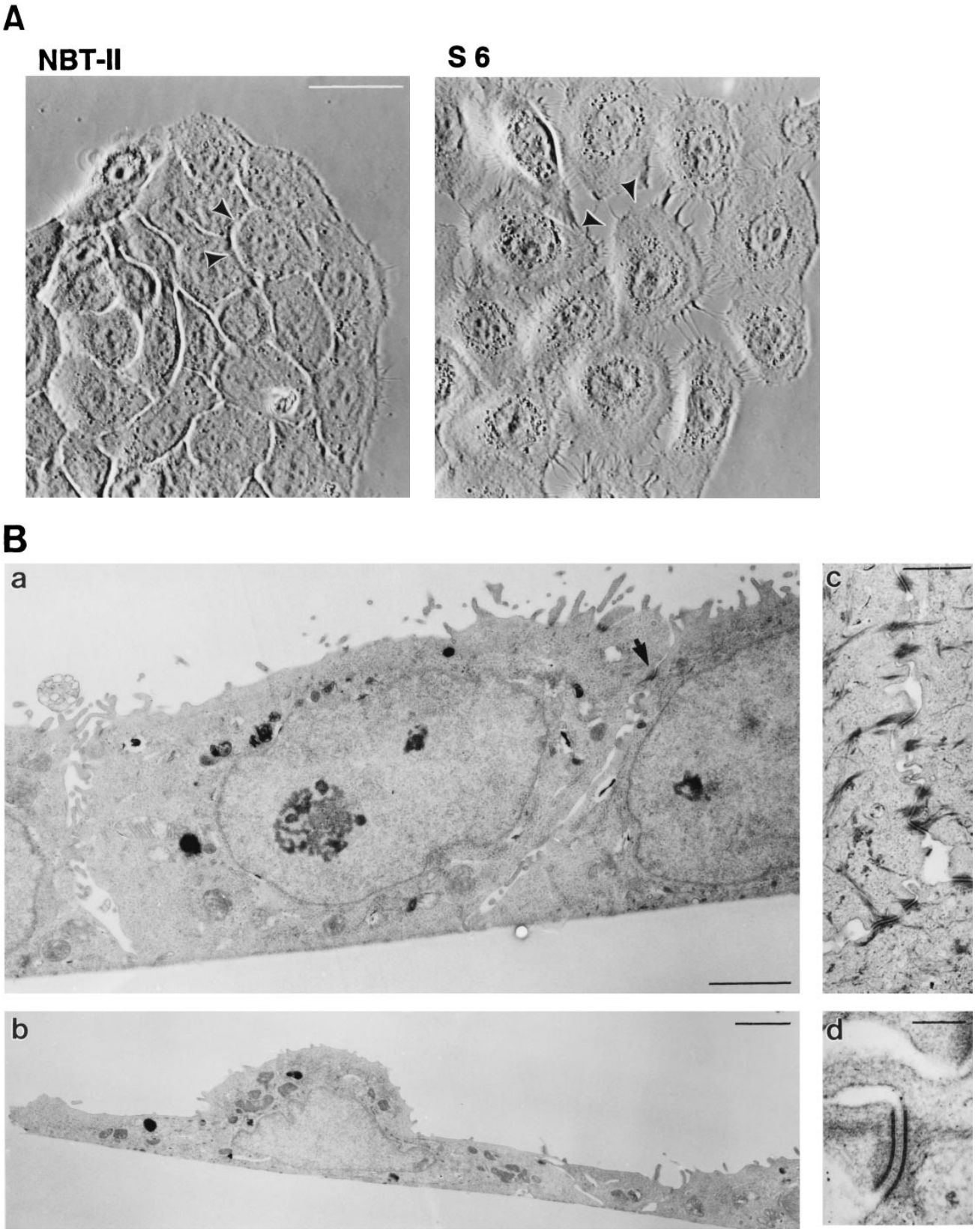

and AS2.10 displayed the typical cobblestone epithelial phenotype expressed by parental NBT-II cells (Fig. 3 *B*).

To check mRNA expression in stable transfectants, Northern analysis was performed using RNA isolated from seven different transfected clones including S3, S4, AS2.8, and AS2.10 clones (Fig. 5). As quantified with a PhosphorImager, transfected clones expressed 10 to 50 times more Slug RNA than parental NBT-II cells (data not shown).

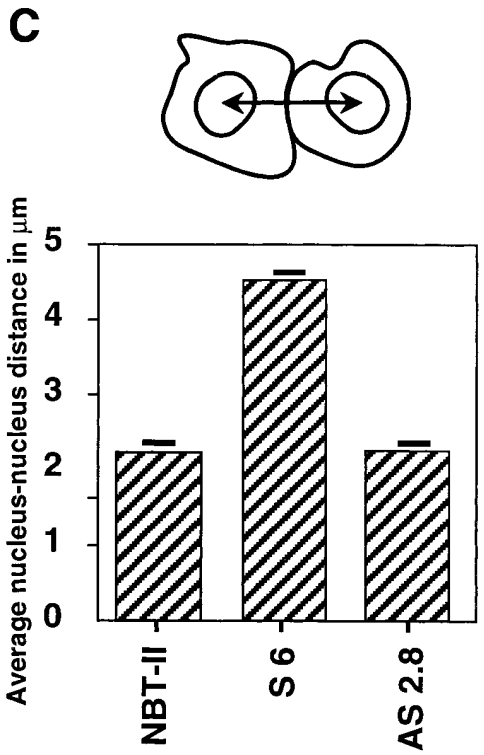

Figure 4. Slug transfectant clone exhibits looser cell contact phenotype. (*A*) NBT-II and S6 cells were observed at higher magnification. Arrowheads indicate cell edges, which are often free for S6 cells compared to involvement in tight cell–cell contacts for control NBT-II cells. (*B*) Electron micrographs of NBT-II cells and S6 cells. NBT-II cells (*a*, *c*, and *d*) or S6 cells (*b*) were plated for 48 h before fixation and processing for electron microscopy. NBT-II cells displayed an epithelial phenotype characterized by numerous desmosomes (*arrow in a*, higher magnifications of other examples in *c* and *d*). Conversely, S6 cells appeared flatter, more spread, and less epithelial. No desmosomes could be found. (*C*) *slug*-transfected S6 cells are more widely spaced in subconfluent cultures than parental NBT-II cells. Cell-to-cell spacing was evaluated by the average distance between the geometrical centers of nuclei of adjacent cells. Only cells in contact with each other were used for the calculation. More than 50 distances were measured in each case to calculate the average nucleus-to-nucleus distance. Bars: (*A*) 10 μm; (*B*, *a* and *b*) 2 μm; (*B*, *c*) 1 μm; (*B*, *d*) 0.2 μm.

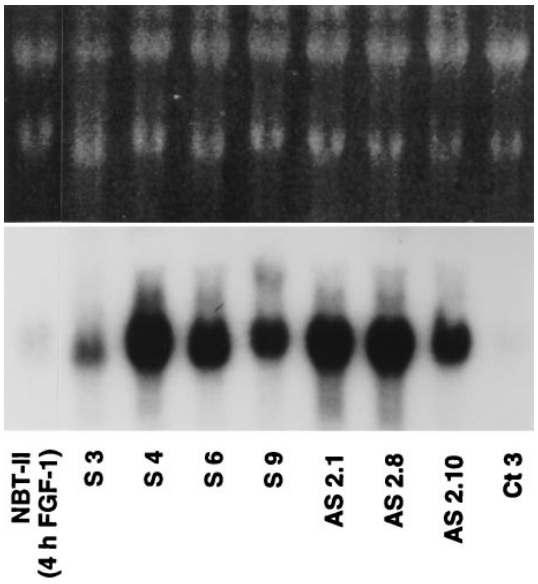

Figure 5. Northern analysis of Slug-mRNA expression by stable transfectants. *slug*-transfected cells expressed large amounts of Slug RNA. Northern analysis using *slug* transfectant clones (sense and antisense) were probed as described for Fig. 2. The double-stranded DNA probe allowed detection of both sense and antisense RNA in the transfectants; Ct 3 was transfected with vector alone.

Expression of Slug Protein in Parental and Transfected NBT-II Cells

We compared the levels of Slug protein in untransfected and transfected NBT-II cells by immunofluorescence using anti–chicken Slug antibodies (Fig. 6). The level of Slug protein expression was very low in parental epithelial NBT-II cells. It was restricted to rare cells that were usually located at the periphery of cell aggregates. After 2 h of FGF-1 treatment, a substantial subpopulation of cells that was also mostly located at the edge of cell aggregates was clearly positive. This population became predominant after 6 h of FGF-1 treatment (Fig. 6). However, after 48 h of FGF-1 treatment and full conversion to a mesenchymal phenotype, Slug protein expression was downregulated.

In contrast, sense-transfected cells expressed Slug before any FGF-1 treatment and maintained it after 6 h of treatment. Antisense-transfected cells did not express Slug before the FGF-1 treatment, and only a few cells located at the periphery of cell aggregates expressed Slug even after 6 h of FGF-1 treatment (Fig. 6).

Immunofluorescence Shows Disruption of Desmosomes in slug-transfected Cells

To analyze potential modulation of desmosomal cell–cell adhesion structures, we localized desmoplakin by immunofluorescence (Fig. 7). To quantitate this modulation, we calculated the percentage of cells displaying desmoplakin localization characteristic of the epithelial phenotype (desmosome-positive) compared to the total number of cells. This ratio was calculated for untreated cells or at different times after FGF-1 treatment for six independent *slug*-transfected clones, and the results are reported in Fig. 7 *B*. Four of these clones, including clones S4 and S6 (Fig. 7 *A*), had a low to null percentage of desmosome-positive cells before any FGF-1 treatment. Cytoplasmic immunoreactivity was found with antidesmoplakin antibodies, suggesting a cytoplasmic desmoplakin pool in S4 and S6 cells. This immunoreactivity was no longer found after 48 h of FGF-1 treatment (Fig. 7 *A* for clone S4; data not shown for S6), as published previously for the parental NBT-II cells (7). In comparison, control clones (C1, C2, and C3) had >95% desmosome-positive cells before treatment, a ratio similar to that for the parental NBT-II cells. In all cases, immunoreactivity was no longer present after prolonged FGF-1 treatment, as published previously for the parental NBT-II cells (7).

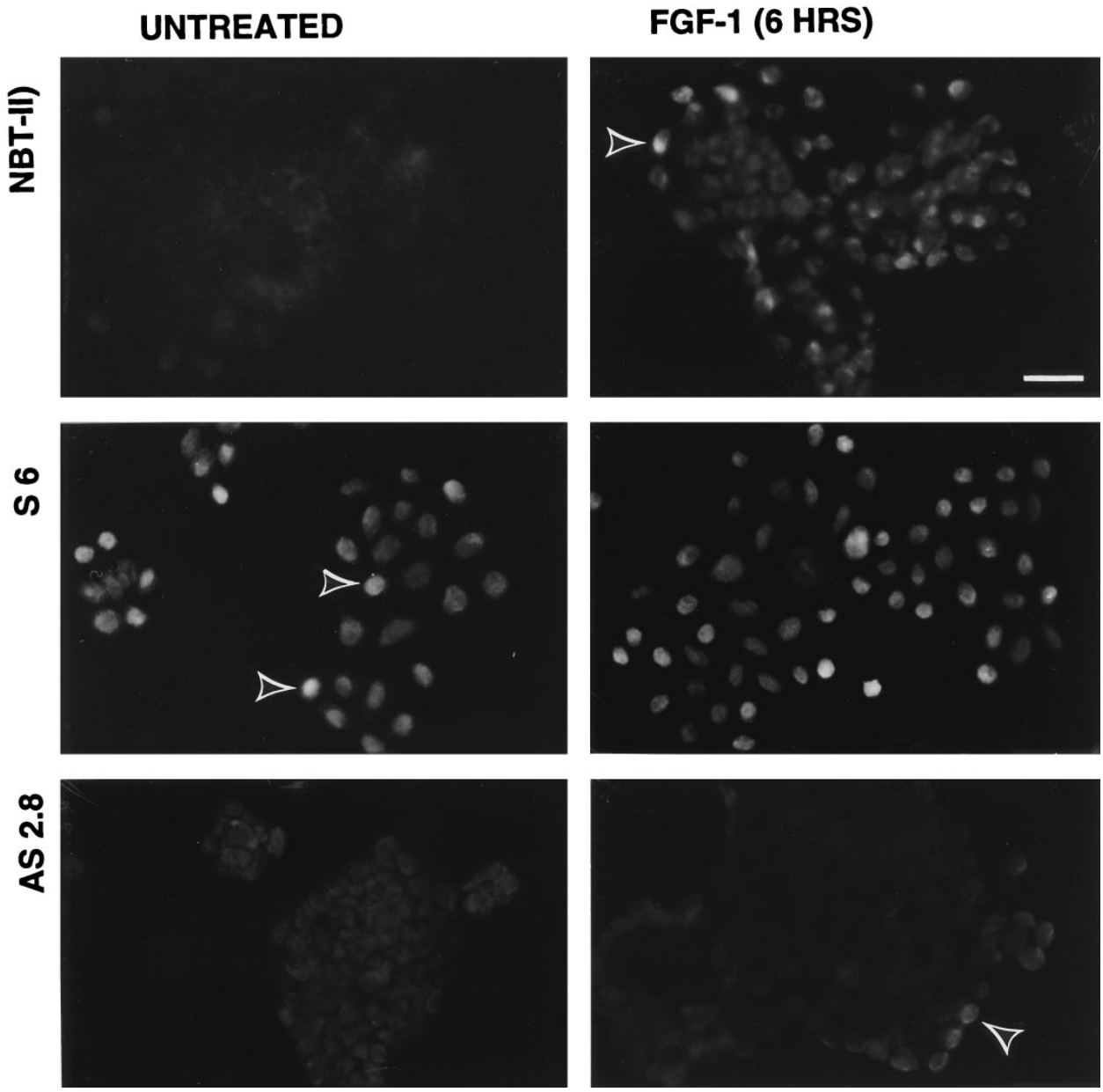

Figure 6. Immunofluorescence analysis of Slug protein expression by transfected and untransfected NBT-II cells. Cells were plated for 24 h and then treated with FGF-1 as indicated. After fixation, cells were immunostained with anti-Slug antibodies. A stable *slug* transfectant clone (S6) and an antisense stable *slug* transfectant (AS2.8) were compared to the parental NBT-II cells. Arrowheads indicate Slug-positive cells. Bar, 35 μm.

Expression of Antisense Slug Inhibits EMT Induced by FGF-1 or HGF/SF

Cells stably transfected with the antisense Slug construct were examined for altered sensitivity to inducers of Slug and EMT. Phase-contrast microscopy showed no significant morphological effects of FGF-1 in these cells (data not shown). Moreover, desmoplakin in desmosomes continued to be localized normally at cell–cell contact areas in antisense-transfected AS2.8 and AS2.10 cells treated with 5 ng/ml FGF-1 (Fig. 7 *C*). The percentage of desmosome-positive cells was determined for seven independent antisense-transfected clones. Five of them showed significant inhibition of FGF-1–induced internalization of desmosomes. In a time-course study, we determined the percentage of desmosome-positive cells at several times after initiation of the FGF-1 treatment for three antisense clones, AS2.1, AS2.8, and AS2.10 (Fig. 7 *D*). Even after 48 h of FGF-1 treatment, >70% of the cells remained clearly epithelial and desmosome-positive in AS2.8 and AS2.10 cells. This high retention of desmosomes should be compared to the very low level of 0.3% desmosome-positive cells observed in control transfectants (Fig. 7 *B*). These results demonstrate inhibition of the entire process of EMT by antisense *slug* transfection.

To confirm that the suppression of EMT was due only to

the antisense Slug, the antisense mouse Slug stable-transfectant AS2.8 cell line was cotransfected with mouse Slug cDNA and marker-truncated IL-2R in a "rescue transfection" attempt. After this transient transfection and 48 h of culture, cells expressing IL-2R (>100) were examined for desmosome expression as previously described. 85 ± 6% of cells cotransfected with the PCR 3 vector alone expressed desmosomes, a proportion similar to that in control AS2.8 cells, whereas only 26 ± 14% of the AS2.8 cells cotransfected with sense Slug cDNA expressed desmosomes, showing a highly significant ($P < 0.001$) decrease in the number of cells expressing desmosomes (Fig. 8).

Finally, we examined for the ability of antisense Slug to block EMT induced by a potent scatter factor, HGF/SF, which was previously described to induce EMT in NBT-II cells as well as in a variety of other epithelial cells (2, 18, 51, 58). Interestingly, the two clones tested, AS2.8 and AS2.10, also resisted HGF/SF action. Double immunofluorescence using antibodies against desmoplakin and cytokeratin clearly indicated a persistence of desmosomes in antisense-transfected cells with retention of cytokeratin filament insertion into points of cell–cell contact rich in desmoplakin (Fig. 9 *A*). Quantitation of desmosome-positive cells showed a pattern of resistance to dissociation similar to that obtained with FGF-1 (Fig. 9 *B*). At higher concentrations of HGF/SF or of FGF-1, more cell dissociation was observed, suggesting a competitive mechanism.

Modulation of Desmosomal Cadherins in slug-transfected Cells

We examined the distribution of two members of the cadherin family involved in most cell–cell adhesion structures. We chose desmoglein, which is a cadherin found specifically in desmosomes, and E-cadherin, a ubiquitous cadherin also present in cell–cell adherens junctions. Desmoglein was found to disappear from cell–cell contact areas very similarly to desmoplakin in *slug*-transfected cells, as reported previously for NBT-II cells treated with FGF-1 to induce EMT (8). In contrast, desmoglein localization persisted in antisense-transfected clone AS2.8, even after FGF-1 treatment (Fig. 10 *A*). E-cadherin immunostaining was previously described to persist in NBT-II cells undergoing EMT, but it became relocalized diffusely over the cell surface (8). We found a similar distribution in untreated *slug*-transfected S4 cells, which showed a partial relocalization of E-cadherin to regions not involved in cell–cell contacts (Fig. 10 *B*, *arrowhead*). FGF-1 treatment did not significantly change this localization, although E-cadherin immunoreactivity appeared significantly decreased overall in association with a decrease in total cell surface area involved in cell–cell contacts. On the other hand, antisense stable transfectant AS2.8 showed little change in total staining compared with untreated NBT-II cells. However, some E-cadherin expression could also be detected in regions not involved in cell–cell contact areas (Fig. 10 *B*).

Slug-transfected Clones Continue to Express Cytokeratin, but Its Organization Is Altered

Cytokeratin protein levels are progressively downregulated in NBT-II cells treated with FGF-1 for several days (8). Since desmosomes are linked to a cytokeratin network in epithelial cells, we studied cytokeratin localization in *slug* transfectants. Both sense and antisense S4 and AS2.8 cells continued to express a dense cytokeratin mesh, indicating that this later step in EMT is not triggered by Slug. However, in accord with the absence of desmoplakin and desmoglein in S4 cells, these *slug*-transfected cells failed to display the typical pattern of cell–cell junctional cytokeratin filaments anchored tightly in desmosomes as was observed in parental NBT-II cells as well as in AS2.8 cells (Figs. 9 and 11). Epithelial NBT-II cells do not express vimentin intermediate filaments until they are treated for several days with FGF-1 (7). Similarly, <5% of the *slug*-transfected S4 cells were found to express vimentin in absence of FGF-1 treatment. This number increased progressively after FGF-1 treatment and exceeded 95% after 3–4 d in culture, similarly to the alteration observed with parental NBT-II cells. In contrast, very few (<1%) of the antisense *slug*–transfected AS2.8 cells expressed vimentin, even after FGF-1 treatment. Two of the latter rare cells are shown by double staining for cytokeratin and vimentin in Fig. 11 *A* and were found to express simultaneously cytokeratin and vimentin filaments. In addition, they clearly express typical cell–cell connecting cytokeratin filaments indicative of functional desmosomes, even though these cells are also synthesizing vimentin.

Video Time-Lapse Analysis of Transfectant Cell Migration

An important characteristic of NBT-II cells expressing vimentin filaments associated with the complete mesenchymal phenotype achieved after FGF-1 treatment is the appearance of a motile phenotype that can be quantified by time-lapse video microscopy (65). We quantified the motility of *slug* transfectants plated on plastic substrates by analyzing video recordings with or without FGF treatment (Fig. 11 *B*). Interestingly, even in the absence of desmosomes, S4 cells did not express a motile phenotype until treated with FGF-1. Only after treatment did they begin migrating similarly to the parental NBT-II cells treated with FGF-1. On the other hand, with or without prior FGF-1 treatment, antisense *slug*–transfected AS2.8 or 2.10 cells did not express any significant motility, in accord with the persistence of desmosomes and cell–cell contacts.

Discussion

In this study, we tested directly whether the newly described zinc-finger protein Slug plays a central role in regulating one or more steps in the process of EMT, using both gain-of-function and loss-of-function approaches. We cloned and sequenced a mouse full-length cDNA encoding *slug*, which has known homologues in chicken and *Xenopus.* We also cloned fragments of human and rat *slug*; sequences from all species were found to be highly conserved. We transfected full-length *slug* cDNA into NBT-II cells to generate transient as well as stable transfectants for testing its function. *Slug* induced a striking total dissociation of desmosomes in NBT-II epithelial cells incorporating the DNA. It also induced increased spreading and separation of these cells, with a doubled average nucleus-to-nucleus distance and a marked decrease in the proportion of

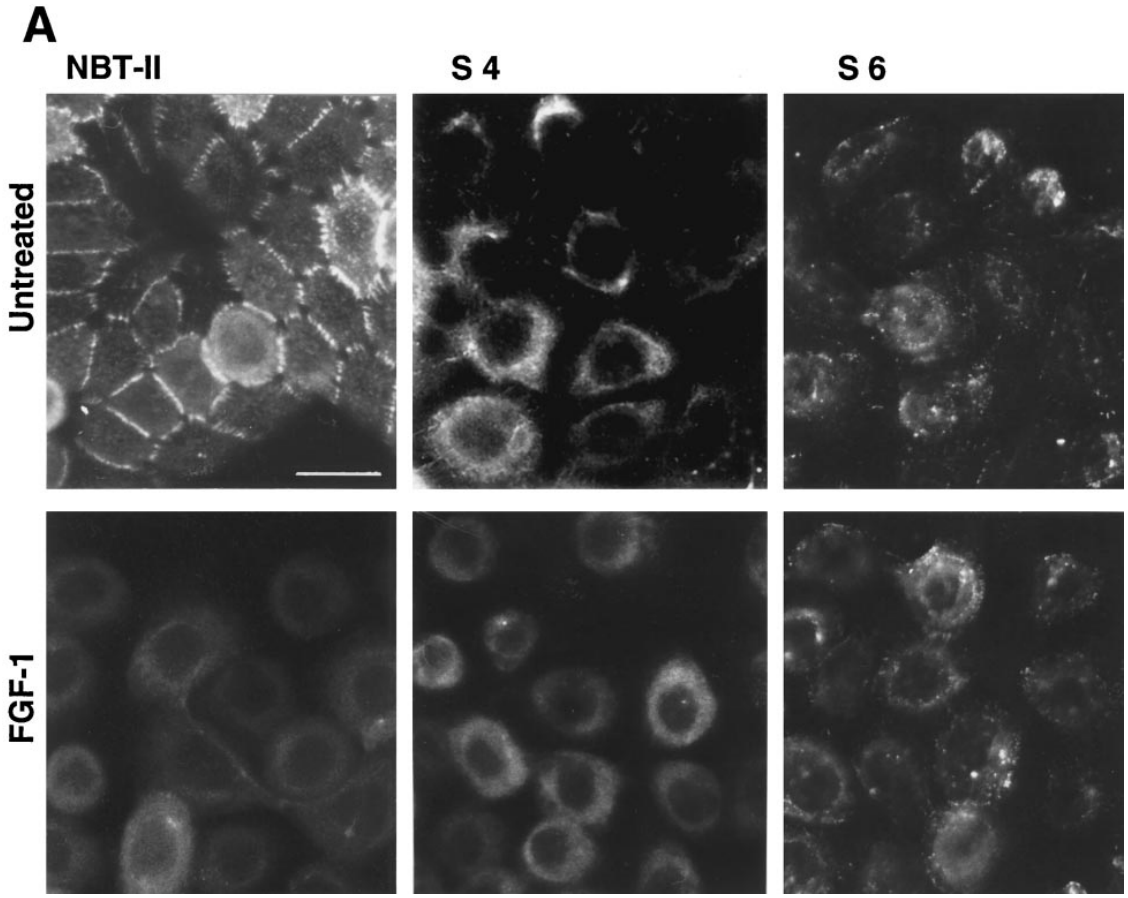

Figure 7. Desmosome expression by *slug*-transfected clones. (*A*) *slug*-transfected NBT-II clones do not express desmosomal structures. Cells were plated for 24 h and then treated with FGF-1 (5 ng/ml) for 48 h in the case of NBT-II cells and S4 cells, and 6 h for S6 cells. After fixation, cells were immunostained with antidesmoplakin antibodies. Two clones of stable *slug* transfectants, S4 and S6, were compared to the parental NBT-II cells. (*B*) Proportion of epithelial cells among FGF-1–treated and –untreated *slug*-transfected NBT-II clones. Cells expressing desmoplakin at cell–cell boundaries (DP^+) were counted after 0 (*nt*), 3, 6, or 48 h of treatment with FGF-1. *slug*-transfected clones (S9, S6, S3, and S4) were compared to control clones C1, C2, and C3 transfected with vector alone. (*C*) Antisense *slug*–transfected NBT-II clones resist FGF-1–induced desmosome dissociation. Cells were plated for 24 h and then treated with FGF-1 (5 ng/ml for 24 h) as indicated. After fixation, cells were incubated with antidesmoplakin antibodies. Two clones of stable antisense *slug* transfectants, AS2.8 and AS2.10, were processed for desmoplakin immunolocalization and photographed at two different magnifications, with or without prior FGF-1 treatment, as indicated. (*D*) Proportion of epithelial cells among FGF-1–treated and –untreated antisense *slug*–transfected NBT-II clones. Cells expressing desmoplakin at cell–cell boundaries (DP^+) were counted after 0 (*nt*), 3, 6, or 48 h of treatment with FGF-1, as indicated. Antisense *slug*–transfected clones (AS 2.1, AS2.8, and AS2.10) should be compared to control clones C1, C2, and C3 transfected with vector alone in *B*. Bars, 10 μm.

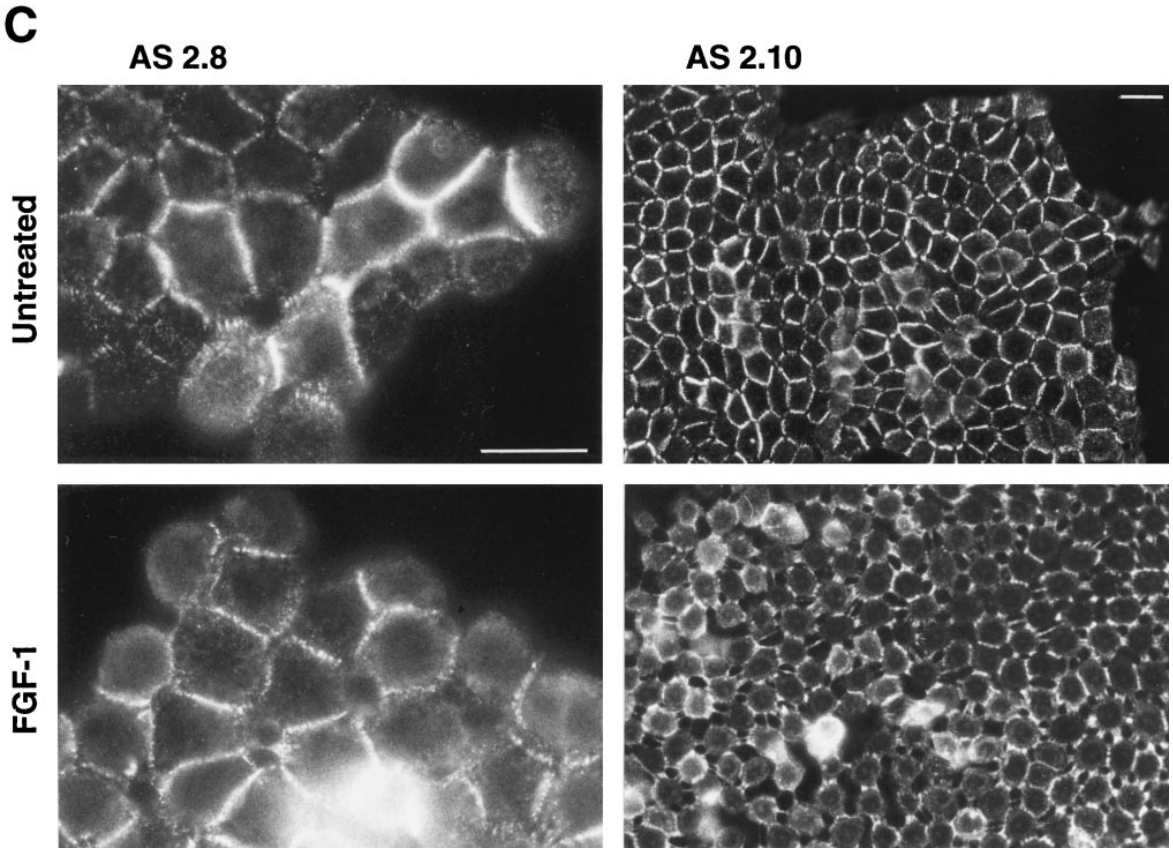

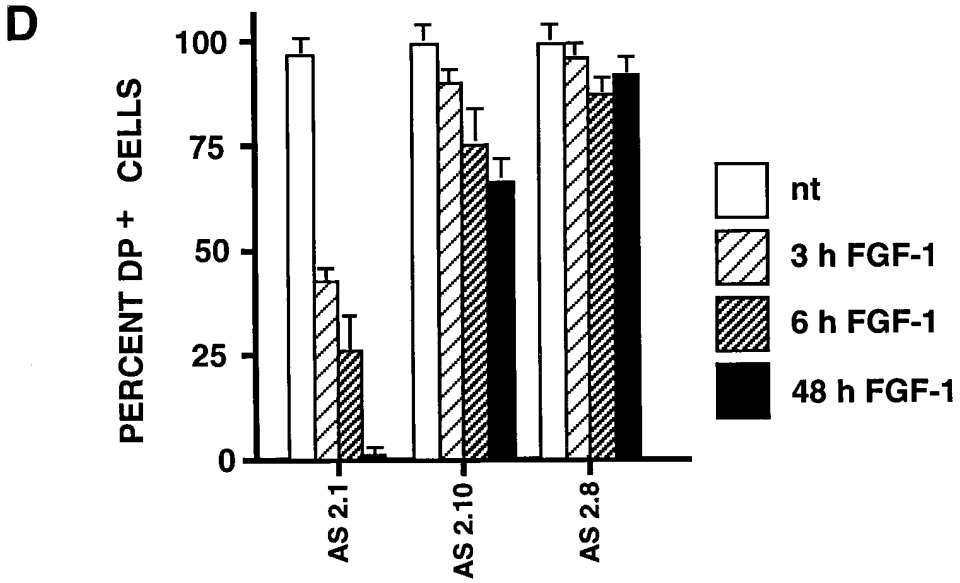

membrane involved in cell–cell contact. Conversely, we found that NBT-II cells transfected with antisense Slug cDNA resisted the actions of both FGF-1 or HGF/SF for inducing desmosomal dispersal and for cell scattering in the EMT process, i.e., antisense *slug* interferes with a necessary Slug expression step in EMT. The specificity of the antisense *slug* activity was supported by a "rescue" *slug* transfection experiment, in which transient overexpression of a *slug* sense construct permitted dissociation of stable antisense transfectants. We conclude from these and other experiments that Slug expression is necessary and sufficient for the first key steps of EMT involving desmosomal dissociation and cell separation, as determined for FGF-induced EMT in NBT-II cells. The resistance of antisense-transfected cells to EMT mediated by FGF-1 as well as HGF/SF suggests that it is a necessary step on which several pathways leading to cell–cell dissociation may converge, initiated by distinct factors such as FGFs or HGF/SF.

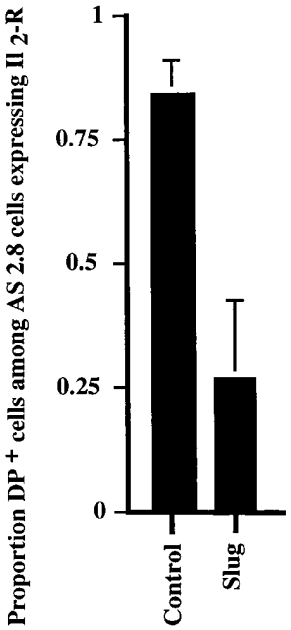

Figure 8. Antisense *slug* stable transfectants can be reverted by transient rescue transfection. Antisense *slug* stable transfectant AS2.8 cells were cotransfected with Slug cDNA and truncated IL-2R. After 48 h culture, >100 cells expressing IL-2R were scored for the presence of desmosomes, as determined by desmoplakin immunolocalization. Cells cotransfected with PCR 3 alone (*Control*) were compared with cells cotransfected with Slug cDNA.

Sequence and Expression Homologies between Chicken, Human, Rat, and Mouse Slug

The full-length sequence of mouse Slug shows 92% amino acid sequence identity to the chicken Slug sequence and 89% identity to *Xenopus* Slug. Interestingly, this homology is much stronger than the homology between mouse and *Xenopus* Snail proteins (initial members of the Snail transcription factor family to which Slug belongs), partially reflecting the disappearance of a zinc-finger motif in the mouse Snail protein. In the DNA segments we cloned and sequenced from other species, mouse Slug showed 100% identity to human Slug in the deduced amino acid sequence and 98% identity to rat Slug. These data, added to the similarity of distribution patterns between chicken and *Xenopus* Slug protein in embryos (42, 46), suggest a conserved function for Slug in vertebrates. Snail is known to be a transcriptional repressor in *Drosophila*, probably acting by direct competition with transcriptional activators (23, 31). A DNA-binding site motif has been defined for the *Drosophila* Snail (41), apparently shared by the related *escargot* gene (14). Escargot was recently described to play a key role during *Drosophila* trachea morphogenesis (60).

It is likely that Slug is also a transcription factor that may recognize specific sites in gene regulatory regions. Snail probably downregulates its own expression through a negative regulatory loop mechanism (41). This could also be the case for Slug, which could explain the transient pattern of expression we observed in NBT-II cells. This transient expression pattern also suggests that Slug initiates a genetic program subsequently dependent on a distinct FGF-1–induced activator. Direct involvement of distinct transcription factors like Ets-1 (66), E1a (21), and c-fos (48) in the induction of cell phenotype modulation, including EMT phases, has been suggested in several cases. However, these factors do not show functional specificity in vivo comparable to that which we describe in the present study of Slug with NBT-II cells.

Slug Targets Desmosomal Proteins

Transient and stable *slug* transfectants showed a characteristic morphological separation of normally tightly apposed plasma membranes at cell–cell boundaries, suggesting that Slug targets some critical cell–cell adhesion system. This separation was accompanied by an increased spreading of the cells well characterized by electron microscopy, resulting in a doubled nucleus-to-nucleus distance. We therefore compared its effects on desmosomal and cadherin-based adhesion systems. Transient and stable transfectants with *slug* showed a disappearance of the desmosomes characteristic of epithelial NBT-II cells. This effect was also found by transient transfections of MDCK cells, a different epithelial cell line normally expressing numerous desmosomes at the cell–cell junctions; although MDCK cells undergo an EMT-like response to HGF but not FGF, Slug can also lead to losses of desmosomes in this cell line (Savagner, P., unpublished data). Desmosome dissociation was observed in most stable transfectant NBT-II clones using three markers. First, desmoplakin and desmoglein, two essential desmosome components, disappeared from cell–cell contact areas. The third desmosomal marker was the focal insertion of cytokeratin filaments, which anchored the desmosomes to the cytokeratin meshwork. The stable transfectant line S4 did express a cytokeratin filament network comparable to parental cells as observed by immunofluorescence, but they did not express any membrane-anchoring cytokeratin filaments. This altered cytokeratin localization pattern was comparable to that observed in epithelial cells transfected with a dominant-negative desmoplakin polypeptide (4). In accord with the immunofluorescence results, Western blot analysis confirmed the presence of desmoglein in untreated Slug transfectants, at a level similar to the untransfected NBT-II cells (Savagner, P., unpublished observation). The three markers were downregulated after several days of FGF-1 treatment, as for the untransfected NBT-II cells (Results and Savagner, P., unpublished observation). Conversely, the three desmosomal markers were positive in *slug* antisense–transfected cells, even after FGF-1 or HGF/SF treatment, demonstrating the continued presence of desmosomes in these cells. Other cell adhesion structures were also investigated. Adherens junction components including E-cadherin and β-catenin (Savagner, P., unpublished observation) were found to be modestly relocalized but still present in S4 cells. They were present as normal in cell–cell contact areas, but they were also present sometimes in membrane regions not involved in cell–cell contacts. This relocalization was mostly present in cells treated with FGF-1. Interestingly, a *slug* antisense stable transfectant exhibited the same relocalization after FGF-1 treatment in spite of the persistence of the desmosomes. This relocalization was very similar to that previously described for E-cadherin on FGF-1–treated NBT-II cells (8). The mechanism of this relocalization of cadherin membrane and intracytoplasmic adhesion molecules and its functional significance are not clear. NBT-II cells were found previously (8) to aggregate similarly via Ca^{2+}- and E-cadherin–dependent mechanisms with or without FGF-1 treatment, suggesting these complexes were indeed functional in spite of the motility of the mesenchymal NBT-II cells. However, the strength of cell–

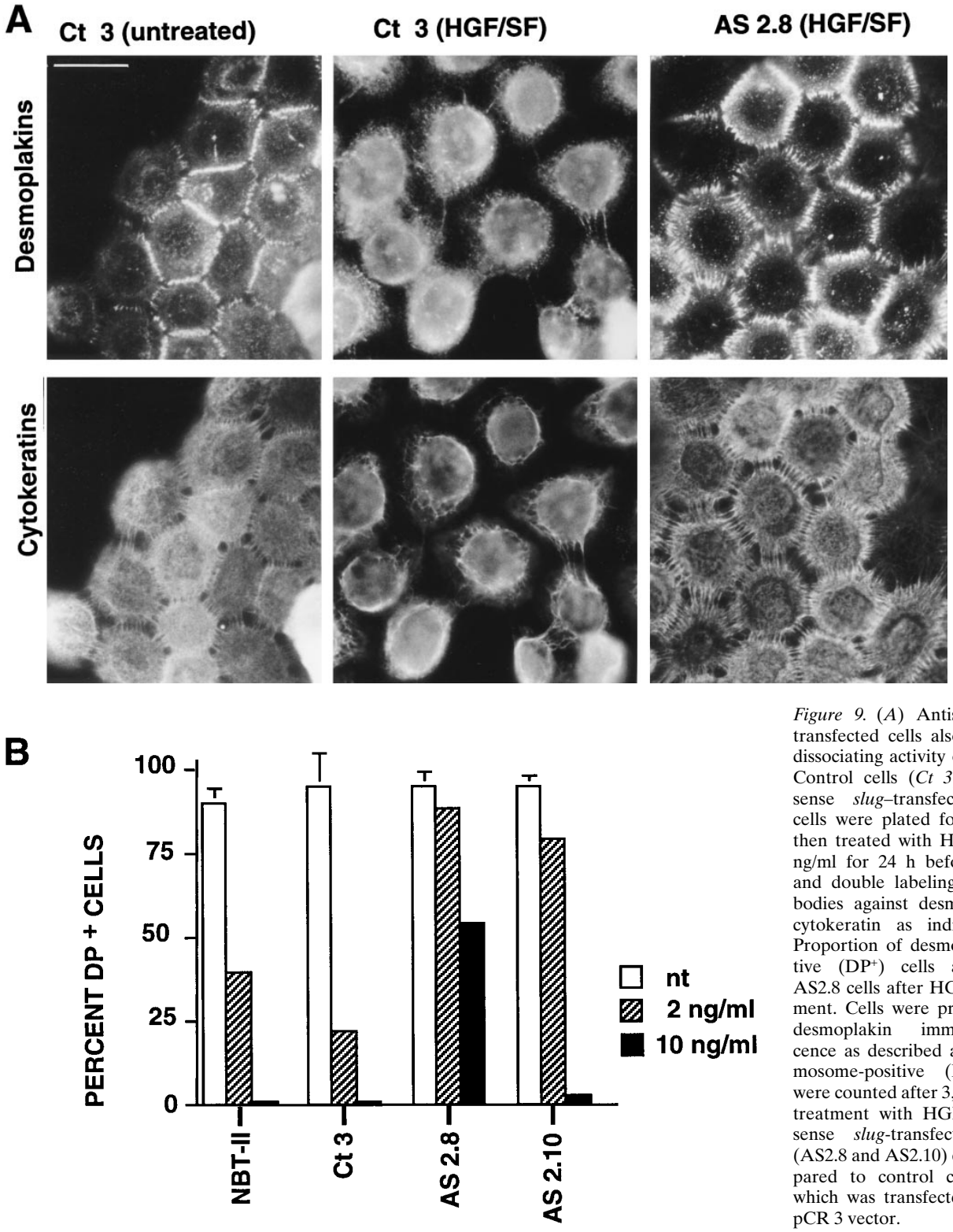

Figure 9. (*A*) Antisense *slug*–transfected cells also resist the dissociating activity of HGF/SF. Control cells (*Ct 3*) and antisense *slug*–transfected AS2.8 cells were plated for 24 h and then treated with HGF/SF at 2 ng/ml for 24 h before fixation and double labeling with antibodies against desmoplakin or cytokeratin as indicated. (*B*) Proportion of desmosome-positive (DP^+) cells among the AS2.8 cells after HGF/SF treatment. Cells were processed for desmoplakin immunofluorescence as described above. Desmosome-positive (DP^+) cells were counted after 3, 6 or 48 h of treatment with HGF/SF. Antisense *slug*-transfected clones (AS2.8 and AS2.10) can be compared to control clone Ct 3, which was transfected with the pCR 3 vector.

cell adhesion might be reduced after such relocalization as in v-src–transfected MDCK cells (59), which would account for the dominant phenotype of Slug-induced cell shape change and cell separation even though components of the E-cadherin system are still present.

Interestingly, this relocalization was not described in epithelial cells transfected with a dominant-negative desmoplakin polypeptide (4), further suggesting that the desmosomes are not the only target for Slug.

Slug Induces the First Phase in the Process of EMT

Our observations suggest that Slug induction triggers the steps of desmosomal disruption, cell spreading, and partial

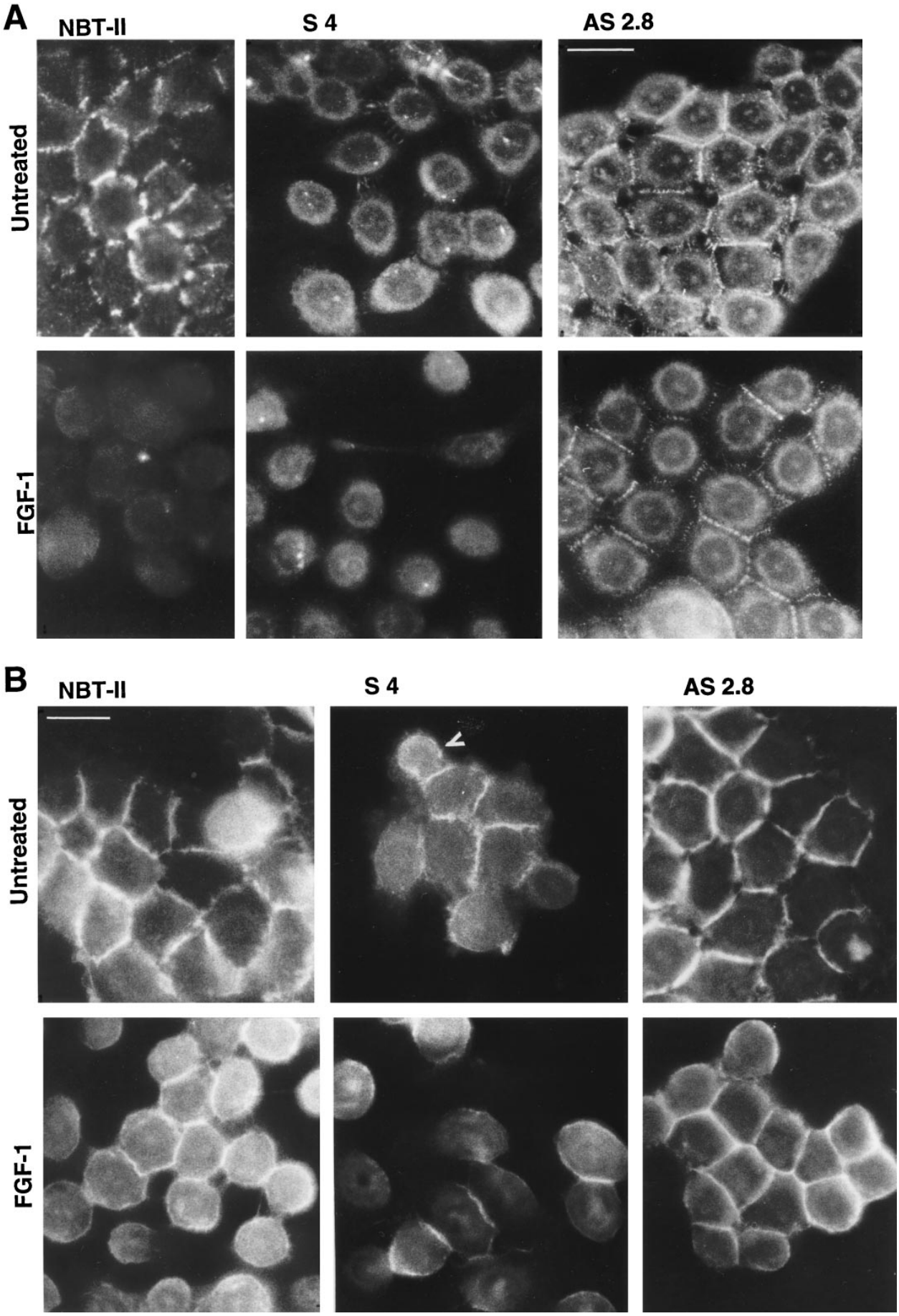
A
NBT-II
S 4
AS 2.8
Untreated
FGF-1
B
NBT-II
S 4
AS 2.8
Untreated
FGF-1

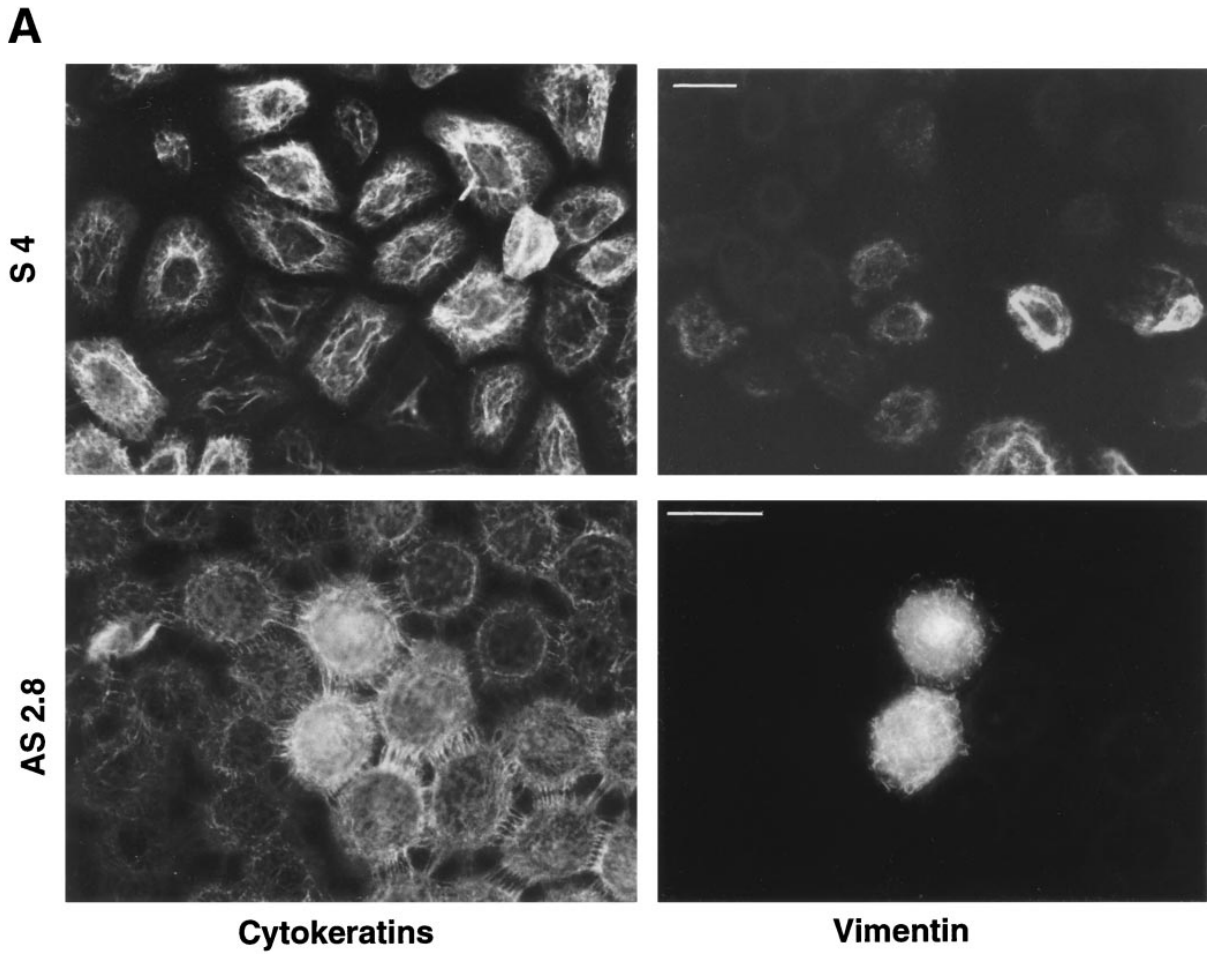

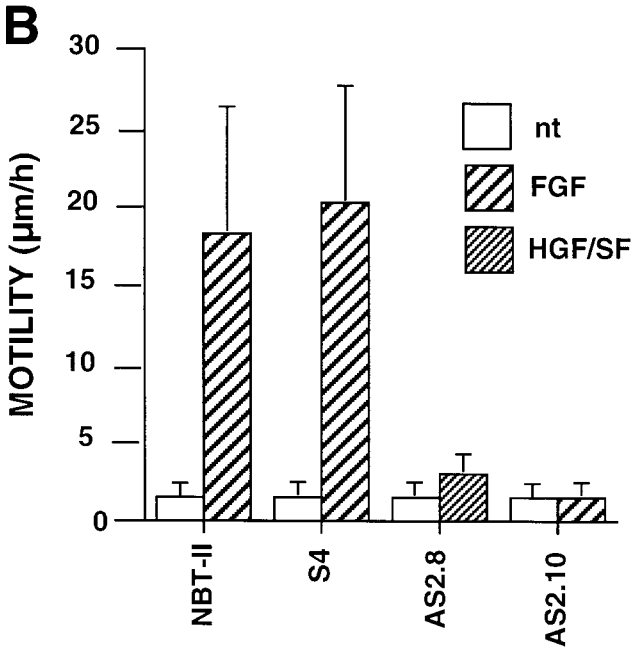

Figure 11. Other processes involved in EMT. (*A*) *slug*–transfected cells display a modified cytokeratin network and require FGF-1 treatment to undergo migration. *Slug* transfectant clone S4 and antisense clone AS2.8 were processed for immunofluorescence as described above after 24 h of culture. In addition, AS2.8 was treated for 48 h with HGF/SF. Cells were labeled with antibodies against cytokeratin or against vimentin as indicated. The AS2.8 cells were double-labeled, and they generally showed little or no reactivity with vimentin antibody, even after HGF/SF treatment. However, shown here is an unusual example of simultaneous expression by two cells of cytokeratin intermediate filaments (including desmosome-connecting filaments) and vimentin intermediate filaments. (*B*) Because initiation of motility often accompanies EMT, NBT-II cell migration after *slug* transfection was evaluated by video time-lapse analysis. Cells were plated for 24 h on culture dishes before a random field was followed for 5 h by time-lapse microscopy. More than 30 cells were individually tracked in each case, and the average of the distances traversed by the cells over 5 h was plotted as the motility. Bars, 10 μm.

Figure 10. Cadherin expression by *slug* transfectants. Stable *slug* transfectants S4 (sense), AS2.8 (antisense), and parental NBT-II cells were prepared for immunofluorescence using antibodies against desmoglein (*A*) or E-cadherin (*B*). Cells were treated with FGF-1 (5 ng/ml) for 24 h as indicated. Bars, 10 μm.

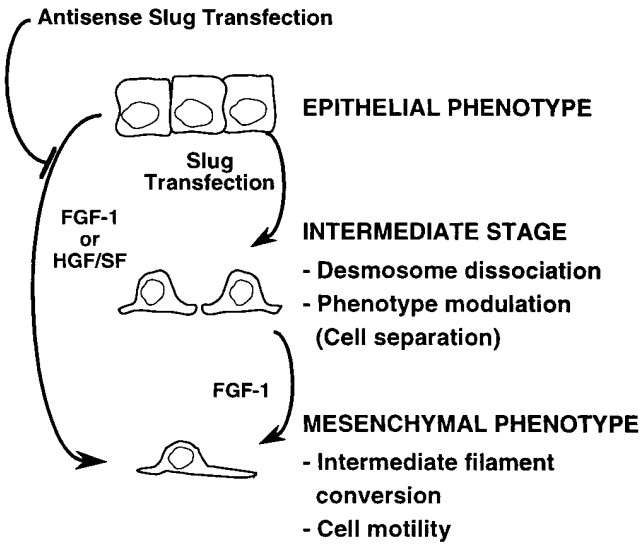

Figure 12. EMT phases. *Slug* transfection induced the transition from epithelial cells to an intermediate phenotype stage characterized by a drastic modulation of the cell–cell adhesion system, including the dissociation of desmosomes. A second stage is postulated to occur when cells are treated with FGF-1, involving the replacement of cytokeratin intermediate filaments by vimentin intermediate filaments and the appearance of cell motility. Both phases are blocked if the first phase is blocked by antisense slug transfection (⊣).

separation at cell–cell borders, which comprise the first and necessary phase of the EMT process in our NBT-II cell model, but that Slug cannot trigger the second phase, which includes the induction of cell motility, repression of the cytokeratin expression, and activation of vimentin expression (Fig. 12). Our studies therefore provide the first demonstration of discrete mechanistic phases in EMT. It is conceivable that the overexpression and the persistence of Slug expression in transfected clones might interfere with a Slug-triggered induction of this second phase. However, additional FGF treatment of such transfectants readily induces this second phase, demonstrating the absence of a block. Therefore, we propose that a distinct mechanism is responsible for the induction of motility in NBT-II cells treated with FGF-1. Such a mechanism is in accord with previous observations analyzing phases in endothelial cell conversion to mesenchymal cells that differentiate into the valves and membranous portion of the atrial and ventricular septum during heart morphogenesis (44, 47). Consequently, EMT appears to be a sequential set of events that involves at least two necessary and distinct phases that can be dissected by gain-of-function and loss-of-function transfection approaches. Our studies provide a mechanistic explanation of the results of previous in vivo experiments in which antisense oligonucleotides targeting Slug were found to interfere with embryonic processes involving EMT as a prelude to subsequent differentiation (46). Slug is essential for initiating growth factor–induced EMT, and its actions include induction of desmosome dissociation and disruption of cell–cell adhesive junction.

We are most grateful to Yoshihiko Yamada (National Institute of Dental Research) for the help with cloning of mouse *slug*. We acknowledge the expert technical assistance of Bill Swain (National Institute of Dental Research) for the electron microscopy. The manuscript was improved by critical reading by Brigitte Boyer, Jacqueline Jouanneau, and Ana-Maria Vallés (Institut Curie).

This work was supported by the Centre National de la Recherche Scientifique, the Association pour la Recherche contre le Cancer (ARC 6465), the Ligue Francaise contre le Cancer (National Committee and Committee of Paris), the National Cancer Institute of the National Institutes of Health (2R01 CA 49417-06), the Philippe Foundation and the Human Frontier Science Program Organization, and the National Institute of Dental Research intramural program.

Received for publication 13 September 1996 and in revised form 18 April 1997.

References

1. Behrens, J., K.M. Weidner, U.H. Frixen, J.H. Schipper, M. Sachs, N. Arakaki, Y. Daikuhara, and W. Birchmeier. 1991. The role of E-cadherin and scatter factor in tumor invasion and cell motility. *EXS.* 59:109–126.
2. Bellusci, S., G. Moens, J.P. Thiery, and J. Jouanneau. 1994. A scatter factor-like factor is produced by a metastatic variant of a rat bladder carcinoma cell line. *J. Cell Sci.* 107:1277–1287.
3. Blay, J., and K.D. Brown. 1985. Epidermal growth factor promotes the chemotactic migration of cultured rat intestinal epithelial cells. *J. Cell. Physiol.* 124:107–112.
4. Bornslaeger, E.A., C.M. Corcoran, T.S. Stappenbeck, and K.J. Green. 1996. Breaking the connection: displacement of the desmosomal plaque protein desmoplakin from cell–cell interfaces disrupts anchorage of intermediate filament bundles and alters intercellular junction assembly. *J. Cell Biol.* 134:985–1001.
5. Bouchey, D., W.S. Argraves, and C.D. Little. 1996. Fibulin-1, vitronectin, and fibronectin expression during avian cardiac valve and septa development. *Anat. Rec.* 244:540–551.
6. Boyer, B., and J.P. Thiery. 1993. Cyclic AMP distinguishes between two functions of acidic FGF in a rat bladder carcinoma cell line. *J. Cell Biol.* 120:767–776.
7. Boyer, B., G.C. Tucker, A.M. Vallés, W.W. Franke, and J.P. Thiery. 1989. Rearrangements of desmosomal and cytoskeletal proteins during the transition from epithelial to fibroblastoid organization in cultured rat bladder carcinoma cells. *J. Cell Biol.* 109:1495–1509.
8. Boyer, B., S. Dufour, and J.P. Thiery. 1992. E-cadherin expression during the acidic FGF-induced dispersion of a rat bladder carcinoma cell line. *Exp. Cell Res.* 201:347–357.
9. Carr, K.E., and P.G. Toner. 1982. Cell Structure. An Introduction to Biomedical Electron Microscopy. Churchill Livingstone, Edinburgh. 388 pp.
10. Cate, R.L., R.J. Mattaliano, C. Hession, R. Tizard, N.M. Farber, A. Cheung, E.G. Ninfa, A.Z. Frey, D.J. Gash, and E.P. Chow. 1986. Isolation of the bovine and human genes for Mullerian inhibiting substance and expression of the human gene in animal cells. *Cell.* 45:685–698.
11. Chomczynski, P., and N. Sacchi. 1987. Single-step method of RNA isolation by acid guanidinium thiocyanate-phenol-chloroform extraction. *Anal. Biochem.* 162:156–159.
12. Demlehner, M.P., S. Schafer, C. Grund, and W.W. Franke. 1995. Continual assembly of half-desmosomal structures in the absence of cell contacts and their frustrated endocytosis: a coordinated Sisyphus cycle. *J. Cell Biol.* 131:745–760.
13. Fleming, T.P., Q. Javed, J. Collins, and M. Hay. 1993. Biogenesis of structural intercellular junctions during cleavage in the mouse embryo. *J. Cell Sci.* 17(Suppl.):119–125.
14. Fuse, N., S. Hirose, and S. Hayashi. 1996. Determination of wing cell fate by the *escargot* and *snail* genes in *Drosophila. Development (Camb.).* 122: 1059–1067.
15. Garrod, D.R. 1993. Desmosomes and hemidesmosomes. *Curr. Opin. Cell Biol.* 5:30–40.
16. Geimer, P., and E.G. Bade. 1991. The epidermal growth factor-induced migration of rat liver epithelial cells is associated with a transient inhibition of DNA synthesis. *J. Cell Sci.* 100:349–355.
17. Gherardi, E., and M. Stoker. 1991. Hepatocyte growth factor–scatter factor: mitogen, motogen, and met. *Cancer Cells.* 3:227–232.
18. Gherardi, E., M. Sharpe, K. Lane, A. Sirulnik, and M. Stoker. 1993. Hepatocyte growth factor/scatter factor (HGF/SF), the c-met receptor and the behaviour of epithelial cells. *Symp. Soc. Exp. Biol.* 47:163–181.
19. Gilbert, S.F. 1994. Developmental Biology. Sinauer Associates, Sunderland, MA. 894 pp.
20. Giordano, T., T. Howard, H.J. Coleman, K. Sakamoto, and B.H. Howard. 1991. Isolation of a population of transiently transfected quiescent and senescent cells by magnetic affinity cell sorting. *Exp. Cell Res.* 192:193–197.
21. Gopalakrishnan, S., and M.P. Quinlan. 1995. Modulation of E-cadherin localization in cells expressing wild-type E1A 12S or hypertransforming mutants. *Cell Growth Differ.* 6:985–998.
22. Gospodarowicz, D., and J. Cheng. 1986. Heparin protects basic and acidic

FGF from inactivation. *J. Cell. Physiol.* 128:475–484.
23. Gray, S., P. Szymanski, and M. Levine. 1994. Short-range repression permits multiple enhancers to function autonomously within a complex promoter. *Genes Dev.* 8:1829–1838.
24. Handel, M.A., and L.E. Roth. 1971. Cell shape and morphology of the neural tube: implications for microtubule function. *Dev. Biol.* 25:78–95.
25. Hartmann, G., L. Naldini, K.M. Weidner, M. Sachs, E. Vigna, P.M. Comoglio, and W. Birchmeier. 1992. A functional domain in the heavy chain of scatter factor/hepatocyte growth factor binds the c-Met receptor and induces cell dissociation but not mitogenesis. *Proc. Natl. Acad. Sci. USA.* 89:11574–11578.
26. Hatzfeld, M., G.I. Kristjansson, U. Plessmann, and K. Weber. 1994. Band 6 protein, a major constituent of desmosomes from stratified epithelia, is a novel member of the armadillo multigene family. *J. Cell Sci.* 107:2259–2270.
27. Hay, E.D. 1995. An overview of epithelio-mesenchymal transformation. *Acta Anat.* 154:8–20.
28. Hay, E.D., and A. Zuk. 1995. Transformations between epithelium and mesenchyme: normal, pathological, and experimentally induced. *Am. J. Kidney Dis.* 26:678–690.
29. Heid, H.W., A. Schmidt, R. Zimbelmann, S. Schafer, S. Winter-Simanowski, S. Stumpp, M. Keith, U. Figge, M. Schnolzer, and W.W. Franke. 1994. Cell type-specific desmosomal plaque proteins of the plakoglobin family: plakophilin 1 (band 6 protein). *Differentiation.* 58:113–131.
30. Jackson, B.W., C. Grund, S. Winter, W.W. Franke, and K. Illmensee. 1981. Formation of cytoskeletal elements during mouse morphogenesis. II. Epithelial differentiation and intermediate-sized filaments in early postimplantation embryos. *Differentiation.* 20:203–216.
31. Jiang, J., and M. Levine. 1993. Binding affinities and cooperative interactions with bHLH activators delimit threshold responses to the dorsal gradient morphogen. *Cell.* 72:741–752.
32. Kimelman, D., and M. Kirschner. 1987. Synergistic induction of mesoderm by FGF and TGF-β and the identification of an mRNA coding for FGF in the early *Xenopus* embryo. *Cell.* 51:869–877.
33. Klein, G., M. Landegger, R. Timpl, and P. Ekblom. 1988. Role of laminin A chain in the development of epithelial cell polarity. *Cell.* 55:331–341.
34. Koch, P.J., and W.W. Franke. 1994. Desmosomal cadherins: another growing multigene family of adhesion molecules. *Curr. Opin. Cell Biol.* 6:682–687.
35. Kouklis, P.D., E. Hutton, and E. Fuchs. 1994. Making a connection: direct binding between keratin intermediate filaments and desmosomal proteins. *J. Cell Biol.* 127:1049–1060.
36. LaFlamme, S.E., L.A. Thomas, S.S. Yamada, and K.M. Yamada. 1994. Single subunit chimeric integrins as mimics and inhibitors of endogenous integrin functions in receptor localization, cell spreading and migration, and matrix assembly. *J. Cell Biol.* 126:1287–1298.
37. Lee, H., and G.W. Kalmus. 1976. Effects of cytochalasin B on the morphogenesis of explanted early chick embryos. *Growth.* 40:153–162.
38. Leptin, M., and B. Grunewald. 1990. Cell shape changes during gastrulation in *Drosophila. Development (Camb.).* 110:73–84.
39. Liem, K.F., G. Tremmi, H. Roelink, and T.M. Jessel. 1995. Dorsal differentiation of neural plate cells induced by BMP-mediated signals from epidermal ectoderm. *Cell.* 82:969–979.
40. Mathur, M., L. Goodwin, and P. Cowin. 1994. Interactions of the cytoplasmic domain of the desmosomal cadherin Dsg1 with plakoglobin. *J. Biol. Chem.* 269:14075–14080.
41. Mauhin, V., Y. Lutz, C. Dennefeld, and A. Alberga. 1993. Definition of the DNA-binding site repertoire for the *Drosophila* transcription factor SNAIL. *Nucleic Acids Res.* 21:3951–3957.
42. Mayor, R., R. Morgan, and M.G. Sargent. 1995. Induction of the prospective neural crest of *Xenopus. Development (Camb.).* 121:767–777.
43. Miettinen, P.J., R. Ebner, A.R. Lopez, and R. Derynck. 1994. TGF-β induced transdifferentiation of mammary epithelial cells to mesenchymal cells: involvement of type I receptors. *J. Cell Biol.* 127:2021–2036.
44. Mjaatvedt, C.H., and R.R. Markwald. 1989. Induction of an epithelial-mesenchymal transition by an in vivo adheron-like complex. *Dev. Biol.* 136: 118–128.
45. Nieto, A.M., M.F. Bennett, M.G. Sargent, and D.G. Wilkinson. 1992. Cloning and developmental expression of Sna, a murine homologue of the *Drosophila* snail gene. *Development.* 116:227–237.
46. Nieto, A.M., M.G. Sargent, D.G. Wilkinson, and J. Cooke. 1994. Control of cell behavior during vertebrate development by Slug, a zinc finger gene. *Science (Wash. DC).* 264:835–839.
47. Potts, J.D., J.M. Dagle, J.A. Walder, D.L. Weeks, and R.B. Runyan. 1991. Epithelial-mesenchymal transformation of embryonic cardiac endothelial cells is inhibited by a modified antisense oligodeoxynucleotide to transforming growth factor β3. *Proc. Natl. Acad. Sci. USA.* 88:1516–1520.
48. Reichmann, E., H. Schwartz, E.M. Deiner, I. Leitner, M. Eilers, J. Berger, M. Busslinger, and H. Beug. 1992. Activation of an inducible c-FosER fusion protein causes loss of epithelial polarity and triggers epithelial-fibroblastoid cell conversion. *Cell.* 71:1103–1116.
49. Rodier, J.-M., A.M. Vallés, M. Denoyelle, J.P. Thiery, and B. Boyer. 1995. pp60$^{c\text{-}src}$ is a positive regulator of growth factor–induced cell scattering in a rat bladder carcinoma cell line. *J. Cell Biol.* 131:761–773.
50. Rosa, F., A.B. Roberts, D. Danielpour, L.L. Dart, M.B. Sporn, and I.B. David. 1988. Mesoderm induction in amphibians: the role of TGF-β2-like factors. *Science (Wash. DC).* 239:783–785.
51. Rosen, E.M., J. Knesel, and I.D. Goldberg. 1991. Scatter factor and its relationship to hepatocyte growth factor and met. *Cell Growth Differ.* 2:603–607.
52. Savagner, P., B. Boyer, A.M. Vallés, J. Jouanneau, and J.-P. Thiery. 1994. Modulations of the epithelial phenotype during embryogenesis and cancer progression. *In* Mammary Tumorigenesis and Malignant Progression. R. Dickson and M. Lippman, editors. Kluwer Academic, Norwell, MA. 229–249.
53. Savagner, P., A.M. Vallés, J. Jouanneau, K.M. Yamada, and J.-P. Thiery. 1994. Alternative splicing in fibroblast growth factor receptor 2 is associated with induced epithelial-mesenchymal transition in rat bladder carcinoma cells. *Mol. Biol. Cell.* 5:851–862.
54. Slack, J.M.W., B.G. Darlington, J.K. Heath, and S.F. Godsave. 1987. Mesoderm induction in early *Xenopus* embryos by heparin-binding growth factors. *Nature (Lond.).* 326:197–200.
55. Smith, D.E., F. Franco del Amo, and T. Gridley. 1992. Isolation of Sna, a mouse gene homologous to the *Drosophila* genes snail and escargot: its expression pattern suggests multiple roles during postimplantation development. *Development (Camb.).* 116:1033–1039.
56. Stappenbeck, T.S., E.A. Bornslaeger, C.M. Corcoran, H.H. Luu, M.L. Virata, and K.J. Green. 1993. Functional analysis of desmoplakin domains: specification of the interaction with keratin versus vimentin intermediate filament networks. *J. Cell Biol.* 123:691–705.
57. Stappenbeck, T.S., J.A. Lamb, C.M. Corcoran, and K.J. Green. 1994. Phosphorylation of the desmoplakin COOH terminus negatively regulates its interaction with keratin intermediate filament networks. *J. Biol. Chem.* 269:29351–29354.
58. Stoker, M., and E. Gherardi. 1989. Scatter factor and other regulators of cell mobility. *Br. Med. Bull.* 45:481–491.
59. Takeda, H., A. Nagafuchi, S. Yonemura, S. Tsukita, J. Behrens, W. Birchmeier, and S. Tsukita. 1995. V-Src kinase shifts the cadherin-based cell-adhesion from the strong to the weak state and β catenin is not required for the shift. *J. Cell Biol.* 131:1839–1847.
60. Tanaka-Matakatsu, M., T. Uemura, H. Oda, M. Takeichi, and S. Hayashi. 1996. Cadherin-mediated cell adhesion and cell motility in *Drosophila* trachea regulated by the transcription factor Escargot. *Development (Camb.).* 122:3697–3705.
61. Thisse, C., B. Thisse, and J.H. Postlethwait. 1995. Expression of snail2, a second member of the zebrafish snail family, in cephalic mesendoderm and presumptive neural crest of wild-type and spadetail mutant embryos. *Dev. Biol.* 172:86–99.
62. Troyanovsky, S.M., L.G. Eshkind, R.B. Troyanovsky, R.E. Leube, and W.W. Franke. 1993. Contributions of cytoplasmic domains of desmosomal cadherins to desmosome assembly and intermediate filament anchorage. *Cell.* 72:561–574.
63. Troyanovsky, S.M., R.B. Troyanovsky, L.G. Eshkind, V.A. Krutovskikh, R.E. Leube, and W.W. Franke. 1994. Identification of the plakoglobin-binding domain in desmoglein and its role in plaque assembly and intermediate filament anchorage. *J. Cell Biol.* 127:151–160.
64. Troyanovsky, S.M., R.B. Troyanovsky, L.G. Eshkind, R.E. Leube, and W.W. Franke. 1994. Identification of amino acid sequence motifs in desmocollin, a desmosomal glycoprotein, that are required for plakoglobin binding and plaque formation. *Proc. Natl. Acad. Sci. USA.* 91:10790–10794.
65. Vallés, A.M., B. Boyer, J. Badet, G.C. Tucker, D. Barritault, and J.P. Thiery. 1990. Acidic fibroblast growth factor is a modulator of epithelial plasticity in a rat bladder carcinoma cell line. *Proc. Natl. Acad. Sci. USA.* 87:1124–1128.
66. Vandenbunder, B., C. Queva, X. Desbiens, N. Wernert, and D. Stehelin. 1994. Expression of the transcription factor c-Ets1 correlates with the occurrence of invasive processes during normal and pathological development. *Invasion Metastasis.* 14:198–209.
67. Zhang, H.Y., M.L. Chu, T.C. Pan, T. Sasaki, R. Timpl, and P. Ekblom. 1995. Extracellular matrix protein fibulin-2 is expressed in the embryonic endocardial cushion tissue and is a prominent component of valves in adult heart. *Dev. Biol.* 167:18–26.
68. Zhou, X., H. Sasaki, L. Lowe, B.L.M. Hogan, and M.R. Kuehn. 1993. Nodal is a novel TGFβ-like gene expressed in the mouse node during gastrulation. *Nature (Lond.).* 361:543–546.